

Influence of the Dynamic Ergodic Divertor on TEXTOR Discharges

K.H. Finken¹, Y. Xu², S.S. Abdullaev¹, M. Jakubowski¹, M. Lehnen¹,
 M. F. M. de Bock³, S. Bozhakov¹, S. Brezinsek¹, C. Busch¹, I.G.J. Classen³,
 J.W. Coenen¹, D. Harting¹, M. von Hellermann³, S. Jachmich², R.J.E. Jaspers³,
 Y. Kikuchi⁴, A. Krämer-Flecken¹, M. Mitri¹, P. Peleman², A. Pospieszczyk¹, D. Reiser¹,
 D. Reiter¹, U. Samm¹, D. Schega¹, O. Schmitz¹, S. Soldatov⁵, B. Unterberg¹,
 M. Van Schoor², M. Vergote², R.R. Weynants², R. Wolf¹, O.Zimmermann¹,
 and the TEXTOR Team

1) Institut für Plasmaphysik, Forschungszentrum Jülich, Association EURATOM/FZJ, Trilateral Euregio Cluster, D-52425 Jülich, Germany, www.fz-juelich.de

2) Laboratoire de Physique des Plasmas / Laboratorium voor Plasmafysica, ERM / KMS, EURATOM Association, Trilateral Euregio Cluster, B-1000 Brussels, Belgium

3) FOM-Institute for Plasma Physics Rijnhuizen, Association EURATOM-FOM, Trilateral Euregio Cluster, PO Box 1207, 3430 BE Nieuwegein, The Netherlands, www.rijnh.nl

4) Department of Electrical Engineering and Computer Sciences, Graduate School of Engineering, University of Hyogo, 2167, Shosha, Himeji, 671-2280 Hyogo, Japan

5) RRC Kurchatov Institute, Nuclear Fusion Institute, Kurchatov Sq. 1 123182 Moscow, Russia

e-mail contact of main author: k.h.finken@fz-juelich.de

Abstract. Experiments with the Dynamic Ergodic Divertor (DED) on TEXTOR are discussed. For the visualization of ergodized magnetic field lines, relativistic runaway electrons are applied. The ergodization causes an enhanced loss rate; this loss is higher for low relativistic electrons than for highly relativistic ones, in good agreement with particle orbit mapping. Another application of the DED-perturbation field is the suppression of ELMs during the limiter H-mode. Since the threshold of the H-mode is only barely exceeded in TEXTOR, the ELM-suppression leads to a reduction of the confinement. A mode of spontaneous density built-up has been found for the TEXTOR-DED as well. This mode is in particular strong for an inward shifted plasma; the built-up has a resonant character with respect to $q(a)$. Langmuir measurements with two probe arrays show a strong influence of the ergodization on the edge values of T_e , n_e and E_r . The properties of edge turbulence and turbulence-driven flux are also profoundly modified.

1. Introduction

The importance of magnetic field stochastization for stability, transport heat and particle control in both tokamaks and stellarators is increasingly recognized. The main aim for proposing ergodization of magnetic fields in tokamaks was the distribution of the power to a large fraction of the walls [1] which is still an issue for large scale steady state fusion devices. In this picture the transport of particle and power was treated as a diffusive process which should lead to a broadening of the scrape-off layer and a widening of the contact zone between plasma and wall. Subsequent experiments at different devices such as TEXT, JFT-2M, Tore Supra and TEXTOR [2, 4, 5, 6, 3], have shown the importance of the open magnetic field lines which intersect the walls and impose again a localized interaction zone between plasma and the walls. This zone of field lines with relatively short connection length is called laminar zone.

The interest in ergodic field grew rapidly beyond its original proposal. It was found that the external perturbation imposes a helical divertor structure and that the required external field for imposing a divertor is about an order of magnitude smaller than for a conventional

poloidal divertor [7]. Typical topics of divertor research were plasma detachment [8], impurity shielding or heat deposition; indirectly linked with the divertor aspect are the confinement improvement [9] and turbulence suppression of large scale turbulent eddies [10], [11]. Another application is the mitigation of edge localized modes (ELMs) [12]. Here, recent experiments show the disappearance of strong low frequency ELMs, while maintaining the H-mode pedestal pressure and thus the plasma confinement [13].

In this article we concentrate on few aspects of the DED plasma only, on the visualization of ergodic structures by runaway electron test particles, on the mitigation of ELMs, on confinement improvements and on the influence on edge turbulence and turbulent transport by the DED.

2. Experimental set up

The main component of the DED is a set of magnetic perturbation coils the purpose of which is to ergodize the magnetic field structure in the plasma edge region; these coils are located inside the vacuum vessel at the high field side of the torus. The set consists of 16 individual coils (4 quadruples) plus two compensation coils. The individual perturbation coils, each winding once around the torus, follow the direction of the equilibrium magnetic field of the plasma edge (i.e. helically); the radial location of enhanced interaction where the helical pitch of the coils exactly matches that of the equilibrium field can be fine-tuned e.g. by varying the plasma current. By this means, a resonant effect of the external perturbation field is obtained on the edge plasma at a pre-selected radius whereby a perturbation current of only 15 kA is sufficient to create a stochastic structure.

The five main perturbation modes are centered at $m/n = 12/4$; this has been selected because it creates only small local perturbations (magnetic islands) and avoids undesired disturbances in the plasma core. By connecting certain perturbation coils, the use of lower m and n is possible, which is of interest for exciting and systematically analyzing modes located deeper inside the torus; these modes are called the $m/n = 6/2$ and $3/1$ base modes. The experiments have shown that the $m/n = 6/2$ base mode is the best scenario for the divertor operation on TEXTOR while the $m/n = 3/1$ base mode is the optimum choice for the study of MHD phenomena such as the excitation of tearing modes.

The DED has the unique feature that the perturbation field is not only static as in most other devices but that it has the option of rotation. To our knowledge only the small research tokamak CSTN [14] at Nagoya University has similar features and - at low perturbation current levels - also the TEXT [15] tokamak. The DED can be operated DC, around 50 Hz or at 7 frequencies in the band from 1 kHz to 10 kHz. At low perturbation current (1.5 kA), the perturbation field can be applied across the whole frequency band of interest for feedback stabilisation experiments.

3. Runaway electrons

A new method to visualize processes due to the ergodization is the detection of runaway electrons as test particles; the runaways are measured by synchrotron radiation, super-thermal electron cyclotron emission (ECE) and hard X-rays from relativistic runaway electrons. ECE and synchrotron radiation are both electromagnetic radiation emitted from the accelerated electrons. ECE is line radiation emitted at the electron cyclotron frequency and at the few first harmonics. In typical plasmas of fusion devices, the ECE radiation is optically thick, i.e. it has a large probability of being re-absorbed. The measurement of optically thick black body radiation is a standard method for the determination of the electron temperature. In runaway discharges, the measured EC-radiation is a factor of 4 to 10 above the thermal level. Since the radiation is emitted perpendicular to the magnetic field lines, the energy of the emitting electrons is at most barely relativistic. A quantitative evaluation of the number of runaways from the ECE intensity is very difficult because of its re-absorption in the plasma.

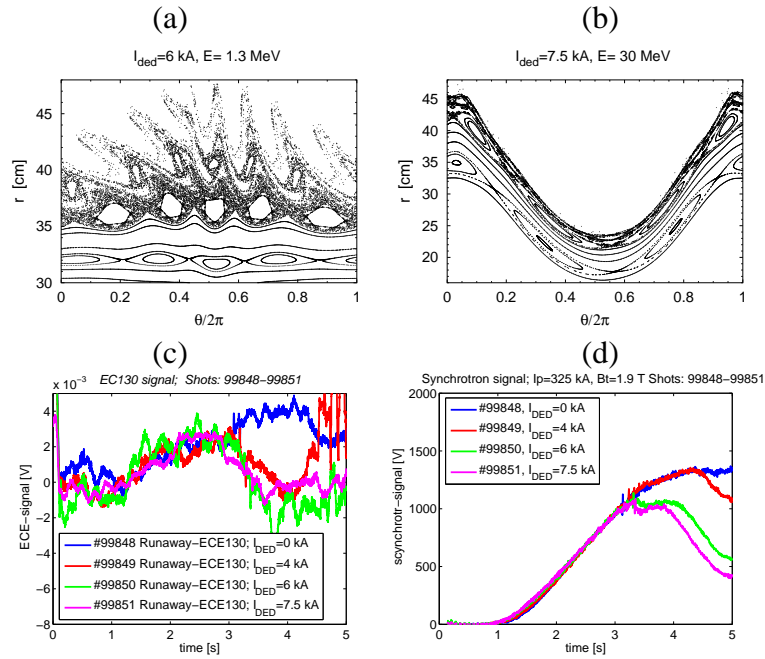


Figure 1: Poincaré plots for the orbits of barely (a) and highly (b) relativistic runaway electrons. With increasing energy, the orbits are strongly shifted to the low field side and the ergodization of the magnetic field lines has less influence on the orbits. Fig. c) shows the traces of the ECE emission from low relativistic electrons for different DED currents and d) the synchrotron radiation of the highly relativistic electrons.

In contrast to ECE, the synchrotron radiation is optically thin and emitted in forward direction of the momentary velocity vector; the opening angle amounts due to the Lorentz-transformation $\theta = 1/\gamma$ where γ is the relativistic mass factor. With increased electron energy, more and more harmonics of the cyclotron frequency are generated forming at relativistic energies a continuous band of radiation. The radiation peak progresses to smaller wavelengths and at the typical maximum TEXTOR runaway energies of $\varepsilon = 25$ MeV to 30 MeV, the emission maximum occurs in the IR spectral range at about $\lambda = 5$ m; at 50 MeV, the radiation would extend to the visible spectral range.

ECE and synchrotron radiation provide information about the low and high relativistic runaways in the plasma. Hard X-rays and neutrons are created when the runaway electrons hit the vessel wall; therefore these data provide information about the runaway loss rate. The threshold for the photo-neutron production amounts to a several MeV runaway electrons.

The orbits of the runaway electrons can be substantially different from the path of the magnetic field lines. Therefore a mapping method has been developed for constructing Poincaré plots of the runaway dynamics. For low relativistic mass factors, the Poincaré plots for the magnetic field and the runaways are practically identical while it deviates strongly for large values of γ . FIG. 1a shows the Poincaré plot of runaway orbits of 1.3 MeV under the influence of the DED field and FIG. 1b is a similar plot for a runaway energy of 30 MeV. The abscissa is the poloidal angle and the ordinate is the minor radius. The low field side corresponds to $\theta/2\pi = 0$ and 1 and the high field side to $\theta/2\pi = 0.5$. One sees a strong ergodization of the orbits near the plasma edge for the "low" energy while only isolated island chains remain for the orbits of highly relativistic electrons. The strong deformation of the flux surfaces in FIG. 1b results from the strong outward shift of runaway electrons with increasing energy.

FIG. 1c) and d) shows the emission of the low relativistic electrons (ECE-signal) and of the highly relativistic ones (synchrotron signal) for different DED currents. In these discharges,

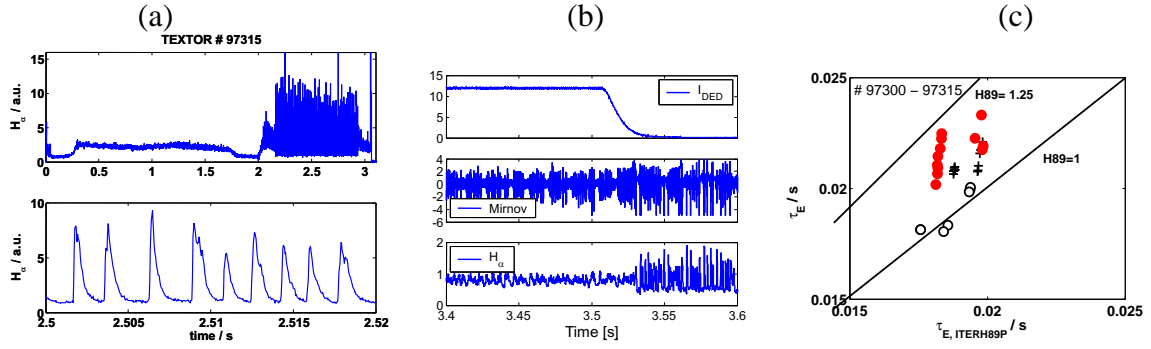


Figure 2: left: a) Time trace of the H_α - signal over the whole discharge (top) and with enhanced time resolution (bottom). middle: b) Mirnov and H_α -signals showing the ELM suppression by the DED. right: c) β_N versus the confinement factor H89 for H-mode (red balls), L-mode (black open circles) and mitigated discharges (crosses).

the DED is ramped up between 3 s and 3.5 s to amplitudes of 0 kA, 4 kA, 6 kA and 7.5 kA. One clearly sees the reduction of the ECE signal for all DED currents $I_{DED} \geq 4$ while the high energy component is not yet affected at $I_{DED} = 4$ (red curves). This is in good agreement with the mapping results. Because of space limitations we cannot present the reduction of radial distribution of the runaways for different DED currents.

4. ELM mitigation

On TEXTOR, special efforts have been started to achieve the limiter H-mode and to study the ELM mitigation by the ergodization field. The H-mode is reached by reducing I_p and B_t ($1T < B_t < 1.4T$; $I_p = 240kA$), shifting the plasma to the high field side applying intense heating; the H-mode threshold amounts to about 1.5 MW to 2 MW depending on the wall conditions. FIG. 2 shows the development of the discharge in the characteristic H_α radiation: Up to 0.6 s I_p and B_t are ramped up to standard values 300 kA / 1.9 T; during the next second, B_t and I_p are ramped down simultaneously to the target value. The heating phase (co & ctr NBI) starts at 2 s. The plasma remains about 200 ms in L-mode and then the ELMs set in. The H-mode threshold is about twice the one of the scaling law for poloidal divertor devices [16] and the ELM frequency amounts to about 500 Hz; increasing slightly with β_N .

FIG. 2b shows the effect of the application of an ergodization field on the ELMs. In this example, the DED current has been switched on before the heating phase and it is ramped down during the heating phase. During the DED-phase, the ELM activity is clearly suppressed. If at first the ELMs are excited and the DED is switched on subsequently, one observes the same effect. The threshold for the DED suppression current is in both cases 3 kA for the DED operating in the $m/n = 12/4$ base mode, i.e. a relatively low DED current. Note, that the suppression of the ELMs occurs in parallel with a reduction of the edge pressure gradient. So far, no conditions could be obtained where the the ELMs are suppressed while the pedestal is maintained.

Therefore, in contrast to the mitigation experiments on type I ELMs of DIII-D [17],[13] show little confinement loss, the edge pedestal in TEXTOR is reduced while the global confinement is only moderately affected. FIG. 2c shows measured energy confinement time as a function of the prediction of the ITERH89-L mode scaling. The H-mode discharges are marked in red while the mitigated examples are the crosses. The crosses are in between the L-mode data and those of the H-mode. We suspect that the obvious reduction of the confinement is due to the fact that the threshold value of the heating power can only barely be exceeded in TEXTOR.

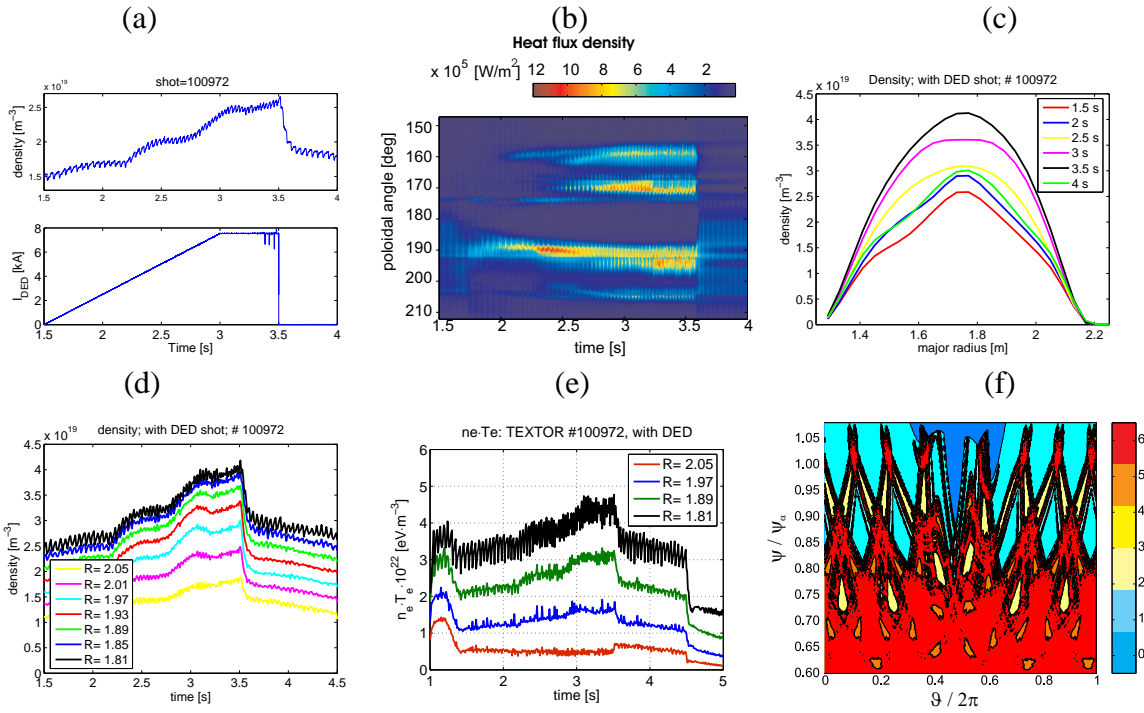


Figure 3: Compilation of data on the spontaneous density built-up mode: a) Time trace of the density (top) and of the DED current (bottom), b) poloidal distribution of the target temperature as a function of time, c) electron density profile development during the DED phase, d) time trace of the electron density, e) time trace of the electron temperature, f) Lamina plot for the strongest confinement at a DED current of 6.3 kA. The magnetic flux tubes from the wall have a relatively short connection length to the $q=2$ surface.

5. Spontaneous density built-up by DED

By varying the edge safety factor of the plasma or the DED-current, it was found that the plasma density increases in a resonant way without gas injection. This density rise is in particular prominent in heated discharges shifted towards the high field side. "Resonant" means that the density increase is observed at certain values e.g. of the plasma current during a current ramp while at other values the density remains or even decreases.

In figure 3 is a compilation of different results is provided. FIG. 3a top shows the increase of the line averaged electron density as a function of time for an optimum q (a) when the DED current is increased (FIG. 3a bottom). It is interesting to see that the electron density increases with DED-current, not linearly but in three distinct steps. Connected with the development of the steps is also a characteristic modification of the footprint pattern (shown is one divertor footprint pair) on the divertor target plates as shown in FIG. 3b [18]: At critical values of the DED current new footprint structures appear which move with increasing away from each other. The footprint pattern has been analyzed theoretically and it is attributed to an opening of deeper and deeper island chains; the opening means that magnetic field lines from the unstable hyperbolic points (X-points) are no longer confined in "sticky" regions in the ergodic area but are connected to the walls. The agreement between theory and experiments is excellent and the deepest island chain which can be touched is the one at the $q=2$ surface. At a higher degree of ergodization, the plasma disrupts.

FIG. 3c shows the electron density profiles at different times during the discharge, time traces of n_e at different radial positions (FIG. 3d) and traces of the electron pressure for the discharge (FIG. 3e). One sees that the density profile increases over the whole profile as well as the stepwise increase of the density. The electron temperature decreases strongly in the

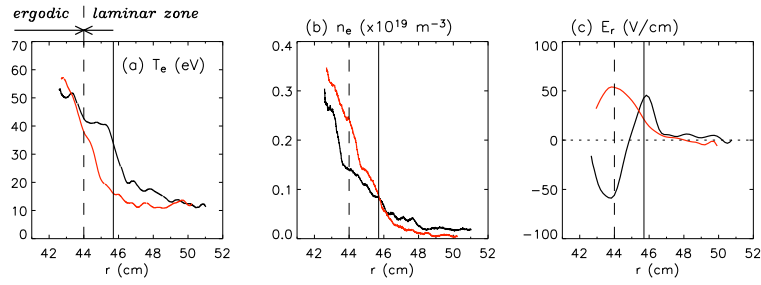


Figure 4: Radial profiles of (a) T_e , (b) n_e and (c) E_r before (black) and during (red) static 6/2 DED. The vertical solid (dashed) line indicates the limiter position (separation of EZ/LZ).

ergodic zone as expected while the decrease in the core is moderate. For this reason the total electron pressure increases over most of the plasma profile and decreases only at the very edge.

We think that the opening of the ergodic field lines toward the wall as seen in the footprints and the stepwise increase of the density are not accidental; we pose the hypothesis that the density built-up is due to a subsequent modification of the electric potential at the resonances $q = 2.5, 2.25$ and 2 . FIG. 3f shows a laminar plot of the lengths of the magnetic field lines in the outer plasma layer for the strong DED current of 6 kA. The colors represent the different connection lengths. One sees, that the orange color penetrates to the surface of $\psi/\psi_a = 0.62$ which corresponds to the $q=2$ surface. This means that the those areas are connected to the walls in less than 2.5 poloidal turns; therefore one would expect an efficient transport of the potential between wall and the $q=2$ surface. The Poincaré plot (not shown here) shows the strong ergodization up to the $q=2$ surface.

6. Turbulence properties

The impacts of the static DED (DC current) on the edge turbulence and turbulent transport have been investigated in various DED scenarios under the following typical discharge conditions: For the $m/n = 12/4$ base mode: $I_p = 250$ kA, $B_T = 1.4$ T, $R/a \simeq 1.73 / 0.46$ [m/m], DED current $I_{DED} = 12$ kA; for 6/2 base mode: $I_p = 270$ kA, $B_T = 1.9$ T, $R/a \simeq 1.73 / 0.46$, $I_{DED} = 6$ kA; and for the 3/1 base mode: $I_p = 250$ kA, $B_T = 1.9$ T, $R/a \simeq 1.75 / 0.48$, $I_{DED} = 1-2$ kA.

The measurements were made by two Langmuir probe arrays installed at the outer mid-plane. The radial extension of the probe measurements covers both the ergodic zone (EZ) and the laminar zone (LZ), the distinction being made by the connection length of field lines, L_c , about 3-4 poloidal turns at the separation locus [3]. Inside the EZ, the Chirikov parameter is larger than 1 and the L_c is longer than the Kolmogorov length, whereas in the LZ the L_c is shorter. In this investigation, the edge equilibrium (fluctuating) electron temperature $T_e(\tilde{T}_e)$, density $n_e(\tilde{n}_e)$ and floating potential $\Phi_f(\tilde{\Phi}_f)$ are detected by a triple probe [19]. The radial electric field E_r is derived from the plasma potential $\Phi_p = \Phi_f + 2.5T_e$ [20]. The turbulent particle flux Γ_{fl} is computed from and fluctuating poloidal electric field (\tilde{E}_Θ) by $\Gamma_{fl} = \langle \tilde{n}_e \tilde{E}_\Theta \rangle / B_\Phi$.

Using the two-point cross-correlation technique [21], the poloidal (radial) fluctuation spectra $S(k, f)$ can be calculated, and hence, the correlation length of turbulence eddies can be estimated from the k spectrum width. The measurements were performed before and during the static DED phases. The results for different DED configurations are quite similar.

FIG. 4 plots the typical equilibrium profiles of T_e , n_e and E_r before and during the static DED. With DED, T_e strongly decreases in the LZ and in the scrape-off layer (SOL), while n_e increases in both the EZ/LZ areas. During DED the E_r changes its sign from negative to positive in most of the LZ and EZ, due to probably the faster moving of electrons than

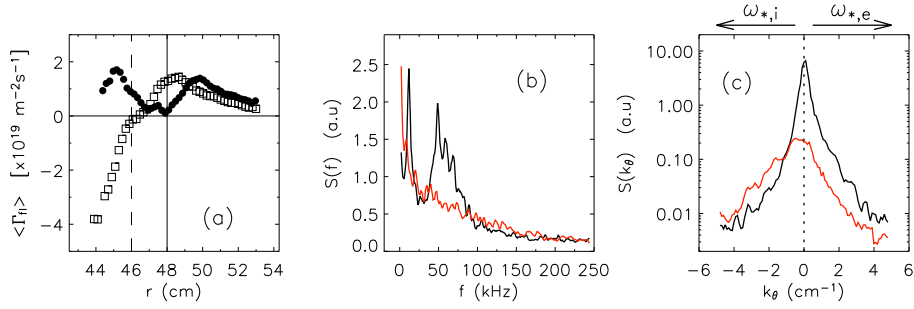


Figure 5: (a) Radial profiles of ensemble-averaged turbulent flux before (balls) and during (squares) static 3/1 DED; (b) $S(f)$ of \tilde{n}_e and (c) $S(k)$ of $\tilde{\Phi}_f$ before (black) and during (red) static 6/2 DED. The $\omega_{*,e}(\omega_{*,i})$ denotes the electron (ion) diamagnetic drift direction.

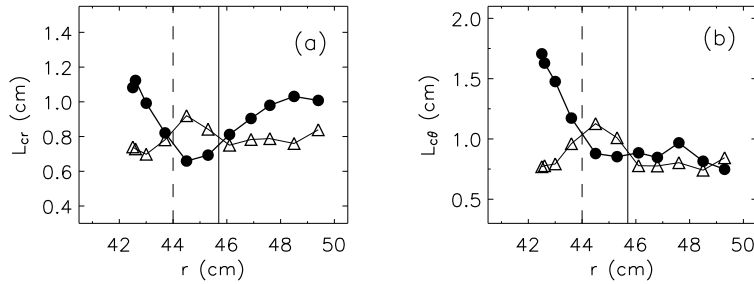


Figure 6: Radial profiles of (a) l_{cr} and (b) $l_{c\theta}$ before (solid balls) and during (open triangles) static 6/2 DED. The vertical solid (dashed) line indicates the limiter position (separation of EZ/LZ).

massive ions along the field lines to the wall. It is noted that the E_r shear is reduced by DED at all radial locations. For fluctuations, the significant changes occur in the EZ, but not in the LZ. Inside the EZ, the fluctuation amplitudes of $\tilde{\Phi}_f$ and \tilde{E}_{θ} are strongly suppressed whereas for \tilde{n}_e the modification is small. An intriguing change is observed on the phase shift between \tilde{n}_e and \tilde{E}_{θ} , which results in a reversal of the Γ_{fl} direction from radially outwards (>0) to inwards (<0), as shown in FIG. 5(a). Further profound changes of the turbulence properties inside EZ can be seen from the frequency and wavenumber spectra, as plotted in FIGS. 5(b) and (c). Before DED for all of \tilde{n}_e , $\tilde{\Phi}_f$ and \tilde{E}_{θ} fluctuations $S(f)$ displays coherent modes with peaks at about 10 kHz and 50 kHz. With DED the modes are all destroyed and $S(f)$ becomes exponential, suggesting an energy redistribution at different frequency components. FIG. 5(c) shows that (i) for small k_{θ} ($-1 < k_{\theta} < 1 \text{ cm}^{-1}$), $S(k_{\theta})$ is largely reduced, indicating a suppression of large scale turbulence structures; (ii) before/during DED, the $S(k_{\theta})$ is power weighted in $\omega_{*,e}/\omega_{*,i}$ direction, implying a change in the poloidal propagation direction of fluctuations, which is indeed consistent with the reversal of the $E_r \times B$ rotation. Shown in FIG. 6 are the radial profiles of l_{cr} and $l_{c\theta}$, i. e., the radial and poloidal correlation length of turbulence eddies. One can clearly see that l_{cr} (and also $l_{c\theta}$) reacts differently to DED in the distinct EZ and LZ area. Inside the EZ, both l_{cr} and $l_{c\theta}$ decrease due to the strong ergodization of field lines, implying a de-correlation effect of DED on turbulence eddies. In contrast, in the LZ, where the magnetic ergodization is no longer efficient, l_{cr} and $l_{c\theta}$ both increase on account of a reduced $E_r \times B$ flow shear in the laminar layer as observed. The results have significant implications for unravelling a controlling role of DED on the edge turbulence.

7. Summary

The DED provides the access a large variety of physics questions. Topics in the past were e.g. the modified edge transport and the resulting effects of the divertor physics, on impurity shielding, on the plasma rotation induced by the perturbation field and on the generation of tearing modes and their suppression by ECRH. This article treats some other recent topics, namely the analysis of enhanced particle losses by runaway electrons, the suppression of ELMs, a scenario of enhanced confinement and the modification of turbulence properties due to the DED-field. It has been found that relativistic runaway electrons can indeed be used as test particles to reveal ergodized magnetic field lines which provide runaway orbits from the confined region to the walls. However, the runaways do not easily reflect the ergodic structure; the orbits depend on the runaway energy: while low relativistic electrons have practically the structure of the field lines, the high relativistic electrons show substantial less ergodization. This trend was verified experimentally.

The suppression of ELMs has been studied on a limiter H-mode on TEXTOR. It is found that a relatively small perturbation field leads to the suppression of the ELMs. Since TEXTOR is underpowered with respect to the limiter H-mode, the edge pedestal in TEXTOR is reduced while the global confinement is only moderately affected.

Ergodization has been introduced in tokamaks for enhancing the plasma transport at the edge in order to distribute the heat flux to a larger area and to reduce the impurity influx. Nevertheless, the ergodization can also establish plasma states with enhanced density built-up. The enhancement is a resonant process and is found for selected values of $q(a)$ and for a strongly inward shifted plasmas. We pose the hypothesis that this mode is related to magnetic flux tubes which connect a relatively deep plasma layer in a short distance with the walls.

Langmuir measurements with two probe arrays show a strong influence of the ergodization on the edge equilibrium profiles and the turbulence properties as well, especially in the ergodic region, where the turbulent flux reverses direction, large scale eddies are suppressed, correlation length is reduced and the turbulence energy redistribution occurs. All of these items indicate a controlling role of the DED on the edge turbulence.

References

- [1] FENEBERG, W. et al., Nucl. Fusion **21** (1981) 669.
- [2] FUCHS, G. et al., Europhysics Conference Abstracts **11D** (1987) 253.
- [3] JAKUBOWSKI, M. W. et al., Phys. Rev. Lett. **96** (2006) 035004.
- [4] MCCOOL, S. C. et al., Nuclear Fusion **30** (1990) 167.
- [5] TAMAI, H. et al., J. Nucl. Mater. **220-222** (1995) 365.
- [6] GHENDRIH, P. et al., Nucl. Fusion **42** (2002) 1221.
- [7] FINKEN, K. H., Nuclear Fusion **37** (1997) 583.
- [8] CONSTANZO, L. et al., J. Nucl. Mater. **290-293** (2001) 840.
- [9] EVANS, T. E. et al., J. Nucl. Mater. **196-198** (1992) 421.
- [10] PAYAN, J. et al., Nuclear Fusion **35** (1995) 1357.
- [11] DEVYNCK, P. et al., Nucl. Fusion **42** (2002) 697.
- [12] TAMAI, H. et al., Proc. 15th Int. Symp. on Plasma Phys, Control. Fusion **1** (IAEA 1995) 137.
- [13] EVANS, T. E. et al., Contrib. Plasma Phys. **44** (2004) 235.
- [14] KOBAYASHI, M. et al., Nucl. Fusion **40** (2000) 181.
- [15] FOSTER, M. S. et al., Nucl. Fusion **35** (1995) 329.
- [16] Kalupin, D. et al., Physics Plasmas **13** (2004) 235003.
- [17] EVANS, T. E. et al., Phys. Rev. Lett. **92** (2004) 235003.
- [18] JAKUBOWSKI, M. W. et al., J. Nucl. Mater. (2007), [to be published].
- [19] CHEN, S. et al., J. Appl. Phys. **36** (1965) 2363.
- [20] STANGEBY, P. C. et al., Nucl. Fusion **30** (1990) 1225.
- [21] BEALL, J. M. et al., J. Appl. Phys. **53** (1982) 3933.